



Developing Geometry Based Criterion Function Method for Predicting Porosity in LM6 Castings

A. Sata^{a,*} , N. Maheta^a , H. Khandelwal^b, S.K. Gautam^b

^aMarwadi University, India

^bDepartment of Foundry Technology, National Institute of Advanced Manufacturing Technology, Ranchi, India

* Corresponding author: E-mail address: amit.sata@marwadieducation.edu.in

Received 24.12.2024; accepted in revised form 06.02.2025; available online 24.06.2025

Abstract

One of the major issues in the metal casting process that affects productivity and energy efficiency is porosity, especially when it comes to castings that are not made in accordance with Original Equipment Manufacturers (OEMs) specifications. Predictive method is crucial to solving this problem. Criterion function is a noteworthy empirical model that has been extensively studied in the literature. By taking into account important factors like cooling rate, thermal gradient and molten metal velocity during solidification, it provides predictive insights into the location and presence of porosity.

It is essential to develop a criterion function that considers the impact of geometric variation on the occurrence of shrinkage porosity. In this paper, a geometry-based model has been proposed for LM6 castings using a standard shape with three T-joints for the prediction of shrinkage porosity. The findings suggest that the presence of joints significantly influences the formation of porosity and it was also observed that an increase in the length ratio leads to a higher occurrence of shrinkage porosity. This information is vital for designers as it guides them to maintain the length ratio within a defined range to prevent shrinkage porosity in T-junction castings.

Keywords: Criterion function, Aluminium alloy-LM6, Shrinkage porosity, Sand casting, Geometric Variation

1. Introduction

The casting sector is consistently working towards enhancing the mechanical characteristics of cast parts [1-3]. Identifying potential defects such as porosity and understanding their influence on material characteristics including elongation to failure, tensile strength and fatigue strength are critical challenges in the quest to produce lighter and higher-performing cast components [4-5]. Gaining insight into these issues will significantly enhance the competitiveness of the aluminum casting industry. The solidification process can lead to two primary types of porosity: shrinkage porosity and gas or air porosity [6]. Porosity is the term

given to interconnected or clustered and an irregular shape related to the shape of the interdendritic region. The development of porosity due to solidification shrinkage commonly referred as a shrinkage porosity poses a significant concern in the metal casting process. The porosity in castings can occur due to gas being released from the liquid metal as it solidifies or due to the inability of the molten metal to flow through the interdendritic space resulting in unfilled gaps.

The production process for casting is intricate with the quality of final product relying on several process parameters. At present, sand casting foundries mainly depend on a "trial and error" method in their design process where the expertise of casting designers is crucial in guaranteeing quality and reducing possible rejection.



Using conventional mathematical calculations, obtaining the best outcomes for casting parameters is difficult [7-9]. To ensure superior casting quality, it is essential to either experimentally adjust casting parameters or employ engineering and production systems such as Computer-Aided Simulation (CAS). Casting simulations take into account practical conditions such as die/mold temperature, pouring temperature and solidification of metal. Casting simulation effectively predicts the solidification pattern, areas prone to shrinkage porosity and evaluating position of casting that impacts porosity formation and prevents shrinkage porosity in metal castings leading to reduced rejection rates, lower energy loss and improved productivity in foundries [10-11]. In the past twenty years, casting simulation and numerical techniques have expanded significantly facilitated by advancements in computer technology.

Casting simulation is basically relied on criterion functions that are derived from thermal parameters. Criteria functions are basic rules that link local cooling rates, solidification and thermal parameters to the possibility of porosity formation. The thermal parameters including temperature, temperature gradient and heat transfer process influence the physical properties of metal and thereby affecting porosity. The simulation addresses various governing equations formulated through the examination of the various physical phenomena associated with metal casting. This approach addresses fundamental equations that depict different physical processes in metal casting including flow, heat transfer, solidification, phase transformation and stress/strain development [12]. These governing equations generally solved by analytical or numerical methods based on intricacy of the process.

Numerous studies have investigated the formation of pores during the solidification stage in various ways. The examination of shrinkage porosity in mold filling and solidification during the sand casting process was carried out by Chudasama [13] using ProCAST software. The research conducted by Ayar et al. [14] involved a casting simulation using AutoCAST-X1 software to explore the behaviors of mold filling and solidification leading to the identification of a shrinkage porosity defect in the central feeder zone. Utilizing the particle method, Naoya Hirata and Koichi Anzai [15] conducted a study to investigate the formation of shrinkage in pure aluminium casting. Properly designing and placing the riser can prevent shrinkage porosity caused by solidifying liquid metal inside it too quickly [16-17].

Several studies have investigated advanced numerical techniques for predicting defects in casting processes, each focusing on different types of imperfections. For instance, one study utilized Darcy's equation to model and forecast the occurrence of shrinkage and gas porosity providing a mathematical approach to these common casting defects [18]. Another research employed the Finite Element Method (FEM) to simulate and predict the distribution of porosity, incorporating critical factors such as the effects of exothermic powders, chills and pads in the casting process [19]. One study demonstrates a method for predicting both the fraction and spatial distribution of micro porosity in Al356 alloy highlighting its influence on interdendritic fluid flow [20]. For example, a technique involving mushy-zone refinement has been utilized to predict pipe shrinkage as well as macro and micro porosity in castings [21]. In another investigation, the Volume of Fluid (VOF) method was employed to simulate and predict the formation and morphology of shrinkage defects [22]. Furthermore, several studies have effectively forecasted the

volumetric fraction of porosity resulting from hydrogen gas precipitation in plate castings [23] and the development of shrinkage porosity in alloys with both short and long freezing ranges [24]. These studies highlight the diversity of methodologies and parameters explored to improve defect prediction and enhance casting quality.

A geometry-driven criterion function has been developed by few researchers, though its application has been primarily limited to a narrow range of alloys. This approach focuses on utilizing geometric parameters related to dimensional ratios to establish predictive models that can evaluate specific properties or behaviour of alloys during processing [25-26]. Although these models show significant promise, their development has primarily focused on a limited subset of alloys. This underscores the necessity for further research to extend their applicability across a broader spectrum of alloy compositions and manufacturing processes. Expanding the scope of these criterion functions is crucial to improve their adaptability and utility in a wide range of industrial contexts.

A comprehensive review of the literature indicates that different criterion functions have been adopted to predict shrinkage porosity formation in castings produced with specific alloy combinations by considering process parameters like cooling rate, thermal gradient and molten metal velocity. Nonetheless, it is necessary to establish criteria functions that consider the impact of geometric variation on shrinkage porosity in LM6 aluminium alloy castings. In this study, a benchmark design consisting of three T junctions was cast and utilized to create a criterion function based on geometric variation for LM6 castings. Actual experimental data, including shrinkage porosity were used to overlay onto simulated results to set up specific simulation parameters. These conditions are also utilized to extrapolate results through casting simulation. The result has been also validated to predict shrinkage porosity using developed geometry-based criterion function.

2. Methodology

Detailed literature review carried out in the direction of development of criterion functions for predicting shrinkage porosity are primarily based on solidification variables related to the thermal gradient and cooling rate during the solidification process. Researchers have extensively established the relationship between these variables and the formation of shrinkage porosity. Consequently, obtaining accurate data on thermal gradients and cooling rates is critical for formulating a reliable criterion function for a specific alloy-process combination. Such data is typically acquired through numerical solutions of governing equations or experimental measurements. Numerical methods demand precise boundary conditions for accuracy while experimental data collection in real-time presents significant challenges. To address these limitations, a hybrid approach is employed combining the strengths of numerical simulations and experimental techniques to better understand solidification phenomena. In this hybrid methodology, experimental results are refined using simulation outcomes. The approach for developing the geometry-driven criterion function is represented in Figure 1 with a stepwise explanation provided in the following section.

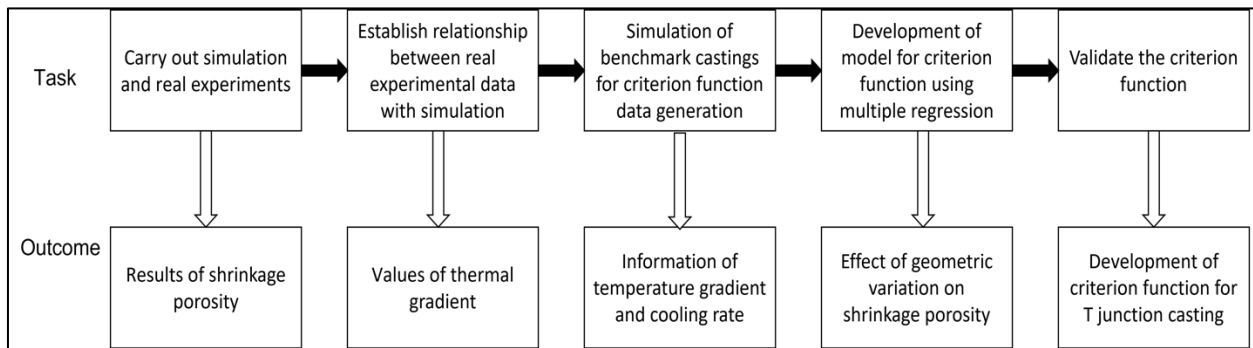


Fig. 1. Methodology for developing a geometry-based criterion function [27]

The steps to developed geometry-influenced criterion function are as follows.

- Benchmark shape is divided into three T – junction
- Geometric variation for benchmark casting
 - T (Arm thickness) = 20 mm (remains constant for each benchmark casting)
 - t (Stem thickness) = 5,10,20,30 (mm)
 - l (Stem length) = 40, 60, 80 (mm)
 - R1 (Thickness ratio) and R2 (Length ratio) as geometric parameters for empirical model development.
 - R1 (Thickness ratio) = t/T (R1 = 0.25, 0.5, 1 and 1.5)
 - R2 (Length ratio) = l/T (R2 = 2, 3 and 4)
- The pore volume of shrinkage porosity was measured for each T-junction in every benchmark casting.
- Create a 3D model and generate the .stl file for each T-junction variation.
- Execute simulation to calculate thermal variables (maximum gradient, maximum temperature, solidification time).
- Determine the maximum gradient for each T-junction using simulation.
- Compute limiting value of gradient (G) with the help of maximum gradient and % limiting value of gradient.
 - Limiting value of gradient (G) = Maximum gradient * (% limiting value of gradient)
- Calculate the solidification time and cooling rate. (r)
 - Cooling rate (r) = (pouring temp. – solidus temp.) / Solidification time (sec).
- Determine the limiting gradient value for each R1 (thickness ratio) and R2 (length ratio) variation of the T-junction through simulation.
- Determine the relationship between R1 (thickness ratio) with the limiting value of gradient (G).
- Repeat the same process for each variation of R2 (length ratio).

3. Design of Benchmark Shape and Experimentation

A benchmark shape with T junctions has been created for testing and developing geometry-based criterion functions for LM6 aluminium alloy through experiments. By connecting three T junctions with different geometric variation, the benchmark shape is produced that has practical applications according to published literature [28]. Achieving this goal involves making proper adjustments to the sectional parameters of the T-junction such as the length and thickness of its elements (like the arm and stem) and the angular orientation of each component about the reference plane.

Every stem thickness (5, 10, 20, and 30 mm) features three levels of arm length variation (40, 60, and 80 mm). This culminates in twelve diverse variations in the sectional elements associated with T-junctions. Two ratios that relate arm thickness to stem length and stem thickness are also considered for future steps. R1 (relationship between stem thickness and arm thickness) and R2 (relationship between stem length and arm thickness) were measured to account for the impact of arm thickness. In general, the arm length remains consistent at 240 mm. The arm length is carefully chosen to allow feeding independence at all three T junctions ensuring that the solidification of one junction remains unaffected by the conditions of the other two junctions. The rationale for choosing independent feeding was to account for the end effect and feeding effect influenced by the casting shape and thickness. Different thickness and length ratio are selected to study the effect of geometric variation on solidification as higher thickness is having lower solidification rate that increases the chances of shrinkage porosity. The sectional orientation remains consistent and is set at 90° (the angle between the arm and the stem). Moreover, it was considered that the radius among stem and arm was minimal to avoid variation of solidification rate and shrinkage porosity. The benchmark shape composed of 3 T junctions is presented in Figure 2 and further detailed in Tables 1 and 2 that outline the values of sectional attributes and their variations.

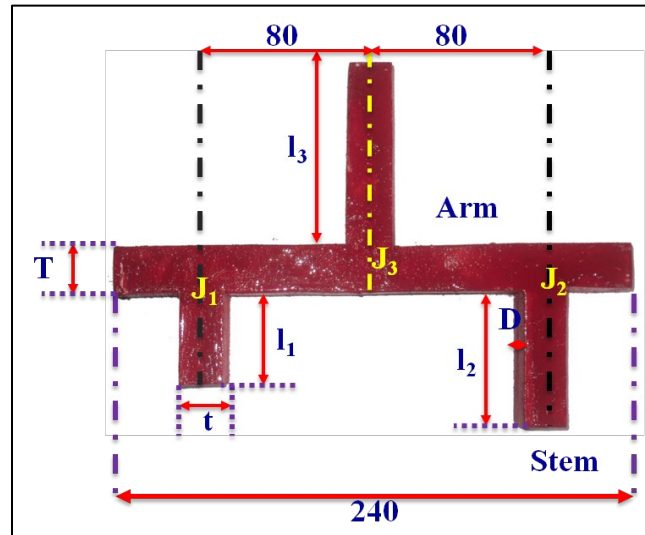


Fig. 2. Benchmark design of shape with 3 T junctions

The studies were conducted with meticulous care to examine shrinkage porosity formation in the sand casting of LM6 aluminium alloy, a material commonly utilized in manufacturing automotive transmission cases. Four experiments were carried out

on a benchmark shape, leading to insights into 12 distinct variations of T-junctions. These variations arose from adjustments in length and thickness ratio highlighting the variation of geometry influence the generation of shrinkage porosity within the junctions.

Table 1.

Input parameters of benchmarks design (dimensions)

Exp. No	Total length of design (L) (mm)	Three different lengths of stems			Arms thickness (T) (mm)	Depth (D) (mm)	Thickness of stems (t) (mm)
		l_1 (mm)	l_2 (mm)	l_3 (mm)			
1	240	40	60	80	20	40	5
2							10
3							20
4							30

Table 2.

Variations in sectional parameters of T junctions in benchmark

Case No.	Junction	Arm thickness T (mm)	Stem thickness (t) mm	Stem length (l_1, l_2 & l_3) mm	Thickness ratio $R_1 = t/T$	Length ratio $R_2 = l/T$	
1	J ₁	20	5	40	0.25	2	
	J ₂			60	0.25	3	
	J ₃			80	0.25	4	
2	J ₁		10	10	40	0.5	2
	J ₂				60	0.5	3
	J ₃				80	0.5	4
3	J ₁		20	20	40	1	2
	J ₂				60	1	3
	J ₃				80	1	4
4	J ₁	30	30	40	1.5	2	
	J ₂			60	1.5	3	
	J ₃			80	1.5	4	

The pattern is prepared from wood and finished with oil paint to enhance the surface quality of benchmark castings as depicted in Figure 1. The design incorporates adjustments for 1% shrinkage, a machining tolerance of 2-5 mm and a draft angle of 1-2 degrees. It was produced by a CNC machine. Figures 3(a) and 3(b) illustrate the cope and drag patterns. To build a green sand mold, silica and bentonite was mixed in the ratio of 10:1. Bentonite is known for its important characteristic of ability to retain water. Furthermore, it is a bonding agent ensuring the sand remains securely in place once the pattern is extracted from the mold box. Detailed information of the mold parameters is represented in Table 3.

Table 3:

Specification of mold box along with sprue, basin and gate	
Dimension of mold boxes (mm)	285 × 285 × 50
Types of mold boxes	Cope and drag
Dimension of sprue (cylindrical) (mm)	D = 20, H = 50
Dimension of pouring basin (square) (mm)	a = 50; Square c/s
Number of gates	2
Number of cavities	1

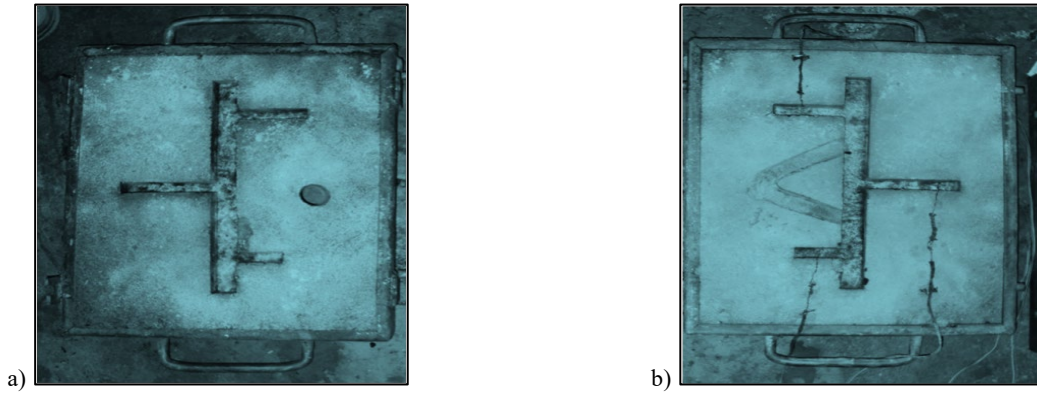


Fig. 3. Mold for benchmark shape of design (a) cope and (b) drag, respectively

The information regarding the chemical composition of the LM6 alloy is provided in Table 4. The alloy was melted in a resistance furnace, reaching a pouring temperature of 700 °C. The molten metal was maintained at a constant temperature for 20 minutes to ensure uniformity. Following the complete homogenization of the molten metal, hexachloroethane (C₂Cl₆) degassing tablets were introduced to the melt for degassing purposes and then the slag was separated from the crucible. Subsequently, the molten metal was poured into a sand mold and allowed to cool at room temperature

followed by removal of casting from mold as shown in figure 4a. During this study, the temperature was determined utilizing a K-type thermocouple. To verify the existence of shrinkage porosity at each junction, parts from the benchmark castings were cut in half horizontally (along the length) 20 mm from the top surface of the castings as shown in figure 4b. The primary objective of splitting the castings in half is to assess the amount of shrinkage porosity and examine how the shape and solidification conditions influence its extent.

Table 4.

Chemical configuration of LM6 alloy

Elements	Si	Cu	Mg	Fe	Zn	Ni	Ti	Mn	Co	Al
Wt.%	10.5	0.1	0.1	0.58	0.1	0.1	0.2	0.5	0.13	Balance

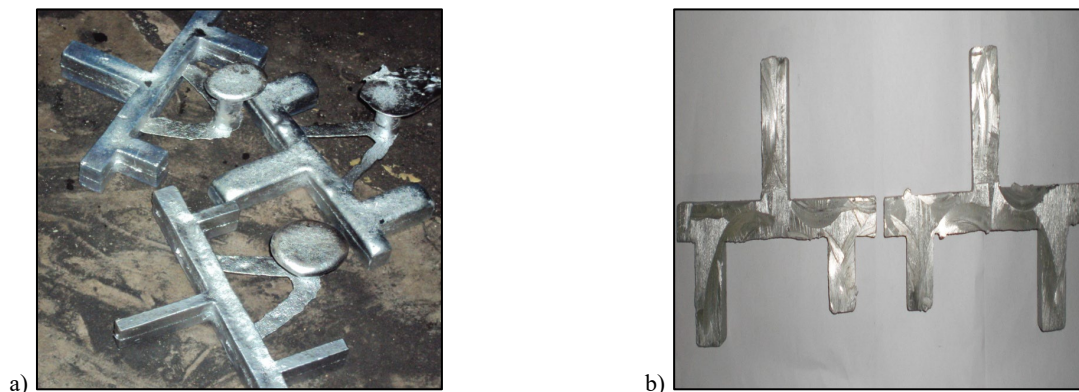


Fig. 4. (a) Cast components and (b) cut section of cast components

4. Simulation

Simulation of the benchmark shape (mentioned as per the different cases in Table 1) was conducted with the simulation software (AutoCAST) to evaluate the potential for shrinkage porosity formation in the designed benchmark shapes. A mesh size of 5 mm was used for both the mold and the surrounding atmosphere while a finer mesh size of 2.5 mm was applied to the casting. Shrinkage porosity in the solidification process can be anticipated through transient thermal analysis using correct initial and boundary conditions. The mold temperature was set at 27 °C initially, while the pouring temperature was set at 700°C. The interfacial heat transfer coefficient for transferring heat between aluminum and silica sand mold is 500 W/m² K and for the transfer between the mold and surrounding air is 11.2 W/m² K assumed to remain constant during solidification. The density of silica sand is 1490 kg/m³ with a thermal conductivity of 0.519 W/m² K and a specific heat of 1170 J/kg. The convergence of simulation was evaluated at 90% of the solidification time. The results obtained

from simulation are represented in figure 5 and further utilized for the development of a criteria function.

The experiments revealed the formation of shrinkage porosity at various junctions with the volume of water occupying each cavity used to measure the extent of shrinkage porosity. To quantify this, a medical syringe was employed to precisely inject a known volume of water into the voids caused by shrinkage porosity. The syringe allowed for accurate measurements with a minimum increment of 0.1 ml enabling precise calculation of the shrinkage porosity volume in the castings.

The findings from the experiments demonstrated that the thickness ratio and length ratio were the primary factors influencing the development of shrinkage porosity. Among the evaluated junctions, junction 3 exhibited the highest degree of shrinkage porosity formation attributed to its larger dimensions compared to the others. The results from both experimental and simulation studies were compiled and presented in Table 5 providing a comprehensive comparison and validation of the findings.

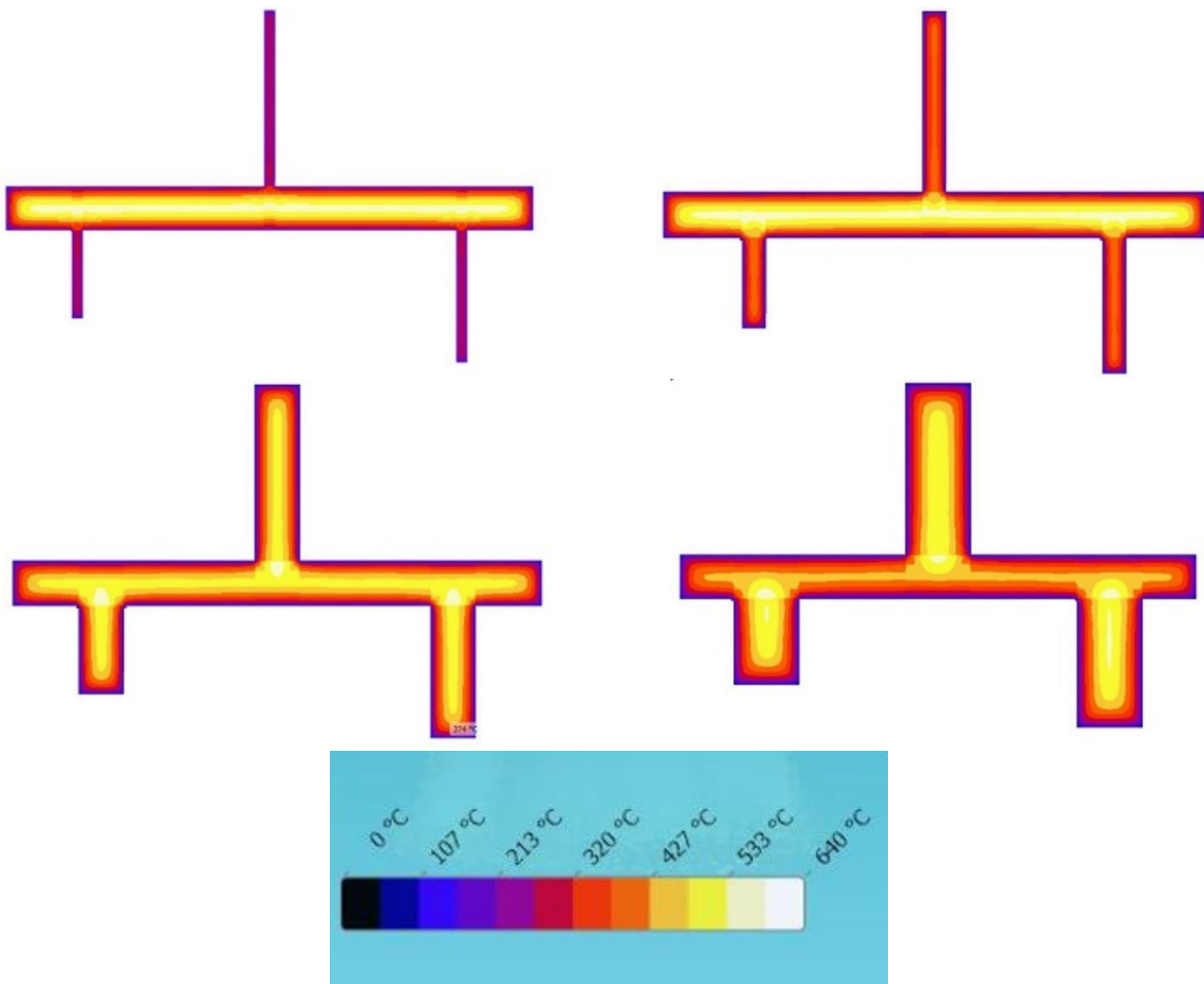


Fig. 5. Simulation of benchmark shape with different cases for LM6 solidification

Table 5.
Experimental and simulation result of shrinkage porosity

Junction	t/T	t	l/T	l	Experiment Shrinkage Porosity (ml of water)	Simulation Shrinkage Porosity (cm3)
1	0.25	5	2	40	0.4	0.4
	0.5	10	2	40	0.45	0.45
	1	20	2	40	0.8	0.79
	1.5	30	2	40	2	2.01
2	0.25	5	3	60	0.55	0.55
	0.5	10	3	60	0.8	0.8
	1	20	3	60	1	1.02
	1.5	30	3	60	2.1	2.16
3	0.25	5	4	80	1	1.05
	0.5	10	4	80	1.6	1.6
	1	20	4	80	2.1	2.12
	1.5	30	4	80	2.2	2.28

5. Harmonizing simulation results with experimental data

Establishing a correlation between real experimental data and simulation results is essential for developing an empirical model capable of accurately predicting shrinkage porosity. Simulation typically relies on inputs related to numerical methods such as time-dependent thermal conductivity, density, and other factors. These inputs lead to small errors into the simulation results. To address this, a correction factor is applied that is determined based

$$\text{Limiting value of thermal gradient (G)} = \text{Thermal gradient max} \times \text{limiting value of thermal gradient \%} \quad (1)$$

$$\text{Cooling rate (r)} = (\text{pouring temperature} - \text{solidus temperature}) / \text{Solidification time} \quad (2)$$

The curve fitting method was employed to determine the correlation between the limiting value of thermal gradient and the thickness ratio. This approach enables the calculation of limiting thermal gradient values for different thickness ratio variations in benchmark castings as outlined in equations 3, 4 and 5. The choice of a third-degree polynomial is primarily acceptable by the statistical metrics obtained during curve fitting such as R-square and adjusted R-square. These values consistently exceeded 0.9 indicating a strong correlation and confirming the polynomial model suitability for the dataset.

$$J1: G = 1.08 - 3.33 R_1 + 4.27R_2^2 - 0.99R_3^3 \quad (3)$$

$$J2: G = 2.18 - 4.82R_1 + 4.45R_2^2 + 0.59R_3^3 \quad (4)$$

$$J3: G = 0.78 + 3.28R_1 + 4.08R_2^2 + 1.54R_3^3 \quad (5)$$

on empirical data. The simulation software provides data on solidification time and the maximum thermal gradient at each point. By analyzing this data, we can determine the critical percentage of the thermal gradient required to match the shrinkage porosity volume observed in experiments with the simulation outcomes. The probability of shrinkage porosity increases with the casting volume. Once this correlation is achieved, determining the limiting values for the thermal gradient and cooling rate using equations 1 and 2 becomes a straightforward process.

6. Development model of criterion function

More data must be generated to gather enough information to develop a criterion function to forecast shrinkage porosity. To achieve this goal, more thickness ratios have been added varying from 0.25 to 1.5 with an increment of 0.05 (the stem thickness is raised by 1 mm for each adjustment) for each T-junction using the length ratio constant at 2, 3, and 4. This leads to 78 variations with 26 thickness ratios (R_1) corresponding to each length ratio (R_2). The criterion function created in this research will include thermal and geometric impacts. The criterion considers maximum thermal gradient, length and thickness ratios and cooling rate. Equations 3, 4, and 5 were used to determine the maximum thermal gradient across all 78 variations. The maximum thermal gradient is tied to the limiting value of the thermal gradient that dictates the percentage of the gradient's limit value. The solidification process was simulated and inputting the percentage limiting gradient and thickness ratio values into a simulation tool resulted in obtaining the shrinkage porosity. The cooling rate data was also extracted

from the simulation. The results for the first junction for different thickness ratio and shrinkage porosity are detailed in Table 6.

Table 6. Output results of developing criteria function related to first junction

Sr no.	R ₁	R ₂	Max. thermal gradient	Limiting value of thermal gradient (G)	limiting value of thermal gradient %	Cooling rate (r)	Porosity
1	0.25	2	4.7	0.293	6.233	0.401	0.400
2	0.30	2	4.7	0.285	6.053	0.401	0.490
3	0.35	2	4.7	0.290	6.170	0.401	0.269
4	0.40	2	4.7	0.308	6.554	0.401	0.271
5	0.45	2	4.7	0.337	7.174	0.401	0.326
6	0.50	2	4.65	0.376	8.086	0.370	0.450
7	0.55	2	4.61	0.423	9.177	0.345	0.516
8	0.60	2	4.59	0.477	10.390	0.322	0.840
9	0.65	2	4.57	0.536	11.732	0.303	0.590
10	0.70	2	4.56	0.599	13.143	0.285	0.622
11	0.75	2	4.56	0.665	14.584	0.285	0.755
12	0.80	2	4.56	0.732	16.048	0.258	0.444
13	0.85	2	4.53	0.798	17.621	0.231	0.420
14	0.90	2	4.42	0.863	19.521	0.221	0.511
15	0.95	2	4.32	0.924	21.395	0.213	0.619
16	1.00	2	4.23	0.981	23.191	0.205	0.800
17	1.05	2	4.15	1.032	24.859	0.197	0.990
18	1.10	2	4.15	1.075	25.899	0.197	1.070
19	1.15	2	4.01	1.109	27.656	0.184	1.710
20	1.20	2	4.01	1.133	28.250	0.184	1.740
21	1.25	2	3.97	1.145	28.837	0.178	1.850
22	1.30	2	3.91	1.144	29.248	0.167	2.070
23	1.35	2	3.99	1.128	28.263	0.163	2.110
24	1.40	2	3.95	1.096	27.738	0.158	2.130
25	1.45	2	3.92	1.046	26.685	0.155	2.110
26	1.50	2	3.91	0.977	25.000	0.151	2.010

Incorporating the geometrical factor, the data are utilized to develop a quantitative prediction model using multiple regression analysis to estimate shrinkage porosity. The regression model's effectiveness is demonstrated in Table 7, with reasonable R-square (above 0.6) and adjusted R-square (in the range of 0.6) values. R-square measures the explanatory power of model by comparing the variance explained by the model to the variance explained by the mean. Adjusted R-square, a modified version of R-square, measures the calculations that prevent a high volume of data points from artificially driving up the measure of explanatory power.

The model's reliability is further validated by its inclusion of parameters such as thickness and length ratios, cooling rate, and satisfactory t-stat and p-values for the limiting thermal gradient. The low p-values highlight the significance of each component, with the thermal gradient (G) being the most influential, followed by the thickness ratio (R₁), cooling rate (r), and length ratio (R₂). A 95% confidence interval was used in developing the model, and the geometry-driven criterion function is expressed in equation 6.

Table 7. Summary of regression analysis

Input parameters	P-values	T-values	Coefficients
Thickness ratio (R ₁)	0.473	-0.72	-0.249
Length ratio (R ₂)	0.010	5.65	0.891
Thermal gradient (G)	0.077	1.79	0.32
Cooling rate (r)	0.083	-1.76	-0.775
R-Square		0.62	
R-Square (Adj)		0.60	

$$\%P = \frac{G^{0.32} \times R_2^{0.89}}{r^{0.76} \times R_1^{0.25}} \quad (6)$$

Where: G: Limiting value of thermal gradient (°C/mm), R₁: Thickness ratio, r: Cooling rate (°C/sec), R₂: Length ratio, %P: The volume of shrinkage porosity expressed as a percentage of the total casting volume (cm³), k = 0.1 (cm⁴/sec)

7. Validation of Criterion Function

To validate the criterion function, shrinkage porosity was measured in a real casting experiment with thickness and length ratios of 1.75 and 5, respectively. The measured shrinkage porosity was approximately 1.6 cm³ (ml of water). Simulation data including cooling rate and maximum thermal gradient were then correlated with the experimental results and applied to the criterion function to predict shrinkage porosity. The predicted porosity volume was 1.84 cm³ reflecting an accuracy higher than 85%. Compared to other models, the proposed approach considers geometric parameters and their variations leading to more accurate and reliable predictions.

8. Conclusions

This study focuses on developing a geometry-based criterion function to predict shrinkage porosity in LM6 castings with T-junctions that are particularly prone to porosity issues. A benchmark casting shape was designed and analyzed emphasizing the critical role of junctions in the occurrence of shrinkage porosity. Experimental data were used to calibrate the simulation tool and additional simulations with varying thickness ratios were conducted to support the development of the criterion function.

The resulting function incorporates the effects of both thickness and length ratios on porosity formation. Testing on T-junction castings demonstrated an accuracy of over 88% highlighting the significant influence of thermal and geometrical factors. This knowledge can assist designers in optimizing length ratios to minimize the risk of shrinkage porosity. The proposed criterion function offers potential enhancements to existing casting simulation tools enabling more accurate predictions of shrinkage porosity in LM6 castings with T-junctions. Additionally, this approach could be expanded to other materials and adapted to predict metallurgical parameters in future research.

Declarations

A. Funding

The authors declare that no funds, grants or other support were received during the preparation of this manuscript.

B. Conflicts of interest/Competing interests

The authors have no relevant financial or non-financial interests to disclose.

C. Availability of data and material

The data that support the findings of this study are available on request from the corresponding author.

D. Ethics approval

Not Applicable

E. Consent to participate

Not Applicable

F. Consent for publication

Not Applicable

References

- [1] Ramesh, S., Gautam, S.K., Roy, H., Lohar, A.K., Samanta, S.K., Anand, A., Mukherjee, D. & Kumar, S. (2024). Structure property correlation of gravity die-cast and rheocast Al–Mg–Sc–Zr in situ Nano-TiB₂ composite. *International Journal of Metalcasting*. 18(4), 3095-103. <https://doi.org/10.1007/s40962-023-01223-2>.
- [2] Khandelwal, H., Gautam, S.K., Ayar, V.S., Upadhyaya, R. & Kumar, A. (2024). Surface modified reinforcements on the structure properties of A356/SiC stir cast composite. *Silicon*. 26, 6269-6276. <https://doi.org/10.1007/s12633-024-03160-z>.
- [3] Gautam, S.K., Roy, H., Chandrakanth, B., Lohar, A.K. & Samanta, S.K. (2024). Effect of processing parameters of rheocast on mechanical properties of Al–10.5 Si–1.7 Cu alloy. *International Journal of Metalcasting*. 18(1), 390-402. <https://doi.org/10.1007/s40962-023-01028-3>.
- [4] Samuel, A.M., Doty, H.W., Valtierra, S. & Samuel, F.H. (2017). Porosity formation in Al–Si sand mold castings. *International Journal of Metalcasting*. 11, 812-822. <https://doi.org/10.1007/s40962-016-0129-0>.
- [5] Tiedje, N.S., Taylor, J.A. & Easton, M.A. (2012). Feeding and distribution of porosity in cast Al–Si alloys as function of alloy composition and modification. *Metallurgical and Materials Transactions A*. 43, 4846-4858. <https://doi.org/10.1007/s11661-012-1308-0>.
- [6] Mohammed, V.M., Arkanti, K. & Ferhathullah, H. (2016). Optimization of sand mould type and melting parameters to reduce porosity in Al–Si alloy castings. *Leonardo Electronic Journal of Practices and Technologies*. 28, 93-106. ISSN 1583-1078.
- [7] Zhao, P., Dong, Z., Zhang, J., Zhang, Y., Cao, M., Zhu, Z., Zhou, H. & Fu, J. (2020). Optimization of injection-molding process parameters for weight control: converting optimization problem to classification problem. *Advances in Polymer Technology*. 1, 7654249, 1-9. <https://doi.org/10.1155/2020/7654249>.
- [8] Cao, L., Liao, D., Sun, F., Chen, T., Teng, Z. & Tang, Y. (2018). Prediction of gas entrapment defects during zinc alloy high-pressure die casting based on gas-liquid multiphase flow model. *The International Journal of Advanced Manufacturing Technology*. 94, 807-815. <https://doi.org/10.1007/s00170-017-0926-5>.
- [9] Shafyey, A., Anijdan, S.M. & Bahrami, A. (2006). Prediction of porosity percent in Al–Si casting alloys using ANN. *Materials Science and Engineering: A*. 431(1-2), 206-210. <https://doi.org/10.1016/j.msea.2006.05.150>.
- [10] Rathod, H., Dhulia, J.K. & Maniar, N.P. (2017). Prediction of shrinkage porosity defect in sand casting process of LM25. *InIOP Conference Series: Materials Science and Engineering*. 225(1), 012237. DOI:10.1088/1757-899X/225/1/012237
- [11] Gautam, S.K., Roy, H., Lohar, A.K. & Samanta, S.K. (2023). Studies on mold filling behavior of Al–10.5 Si–1.7 Cu Al alloy during rheo pressure die casting system. *International Journal of Metalcasting*. 17(4), 2868-2877. <https://doi.org/10.1007/s40962-023-00958-2>.
- [12] Khandelwal, H., Gautam, S.K. & Ravi, B. (2024). Numerical simulation and experimental validation of fluidity of

- AlSi12CuNiMg alloy using multi spiral channel with varying thickness. *International Journal of Metalcasting*. 19, 1202-1211. <https://doi.org/10.1007/s40962-024-01383-9>.
- [13] Chudasama, B.J. (2013). Solidification analysis and optimization using pro-cast. *International Journal of Research in Modern Engineering and Emerging Technology*. 1(4), 9-19. ISSN: 2320-6586.
- [14] Ayar, M.S., Ayar, V.S. & George, P.M. (2020). Simulation and experimental validation for defect reduction in geometry varied aluminium plates casted using sand casting. *Materials Today: Proceedings*. 27(4), 1422-1430. <https://doi.org/10.1016/j.matpr.2020.02.788>.
- [15] Hirata, N. & Anzai, K. (2017). Numerical simulation of shrinkage formation behavior with consideration of solidification progress during mold filling using stabilized particle method. *Materials Transactions*. 58(6), 932-939. <https://doi.org/10.2320/matertrans.F-M2017811>.
- [16] Bekele, B.T., Bhaskaran, J., Tolcha, S.D. & Gelaw, M. (2022). Simulation and experimental analysis of re-design the faulty position of the riser to minimize shrinkage porosity defect in sand cast sprocket gear. *Materials Today: Proceedings*. 1(59), 598-604. <https://doi.org/10.1016/j.matpr.2021.12.090>.
- [17] Choudhari, C.M., Narkhede, B.E. & Mahajan, S.K. (2014). Casting design and simulation of cover plate using AutoCAST-X software for defect minimization with experimental validation. *Procedia Materials Science*. 6, 786-797. <https://doi.org/10.1016/j.mspro.2014.07.095>.
- [18] Kimio, K. & Pehlke, R.D. (1985). Mathematical modeling of porosity formation in solidification. *Metallurgical Transactions*. B16, 359-366. <https://doi.org/10.1007/BF02679728>.
- [19] Chen, Yin-Heng, & Yong-Taek Im, (1990). Analysis of solidification in sand and permanent mold castings and shrinkage prediction. *International Journal of Machine Tools and Manufacture*. 30(2), 175-189. [https://doi.org/10.1016/0890-6955\(90\)90128-6](https://doi.org/10.1016/0890-6955(90)90128-6).
- [20] Sabau, A.S. & Viswanathan, S. (2002). Microporosity prediction in aluminum alloy castings. *Metallurgical and Materials Transactions*. B33 (2), 243-255. <https://doi.org/10.1007/s11663-002-0009-2>.
- [21] Pequet, Ch., Rappaz, M. & Gremaud, M. (2002). Modeling of microporosity, macroporosity, and pipe-shrinkage formation during the solidification of alloys using a mushy-zone refinement method: applications to aluminum alloys. *Metallurgical and Materials Transactions*. A33(7), 2095-2106. <https://doi.org/10.1007/s11661-002-0041-5>.
- [22] Dawei, S. & Garimella, S.V. (2006). Numerical and experimental investigation of solidification shrinkage. *Numerical Heat Transfer, Part A: Applications*. 52(2), 145-162. <https://doi.org/10.1080/10407780601115079>.
- [23] De Obaldia, E. Escobar, & Felicelli, S.D. (2007). Quantitative prediction of microporosity in aluminum alloys. *Journal of Materials Processing Technology*. 191(1-3), 265-269. <https://doi.org/10.1016/j.jmatprotec.2007.03.072>.
- [24] Reis, A., Houbaert, Y., Zhian Xu, Van Tol, R., Santos, A.D., Duarte, J.F. & Magalhaes, A.B. (2013). Modeling of shrinkage defects during solidification of long and short freezing materials. *Journal of Materials Processing Technology*. 202(1-3), 428-434. <https://doi.org/10.1016/j.jmatprotec.2007.10.030>.
- [25] Mazloum, K., & Sata, A. (2024). Development of geometry-driven quantitative prediction for shrinkage porosity in T-junction of steel sand castings. *Turkish Journal of Engineering*. 8(4), 640-646. <https://doi.org/10.31127/tuje.1454237>.
- [26] Sata, A. & Dharaiya, V. (2022). Geometry-driven criterion function for predicting shrinkage porosity in stainless steel castings with T-junction. *Journal of Advanced Manufacturing Systems*. 21(03), 625-38. <https://doi.org/10.1142/S0219686722500226>.
- [27] Sata, A., Maheta, N., Dave, A. & Khandelwal, H. (2025). Geometry based and simulation supported porosity prediction in ductile iron casting. *Engineering Research Express*. 7, 015411, 1-12. DOI: 10.1088/2631-8695/ada71e
- [28] Kamalesh, S., Pavan, R., Durgesh, J., Karupppasamy, S. Ravi, B. (2008). 3D junctions in castings: simulation-based DFM analysis and guidelines. In INAE International Conference on Advances in Manufacturing Technology (ICAMT 2008), 6-8 February 2008.